polymer papers

Neutron reflectometry from stereotactic isomers of poly(methyl methacrylate) monolayers spread at the air–water interface

J. A. Henderson and R. W. Richards*
Department of Chemistry, University of Durham, Durham DH1 3LE, UK

J. Penfold and C. Shackleton
Rutherford–Appleton Laboratory, Chilton, Didcot OX13 0RA, UK

and R. K. Thomas
Physical Chemistry Laboratory, University of Oxford, South Parks Road, Oxford OX1 3QZ, UK
(Received 11 July 1990; revised 16 October 1990; accepted 16 October 1990)

Surface pressure–area isotherms on poly(methyl methacrylate) 'monolayers' spread at the air–water interface show that the isotactic polymer is in good solvent conditions, whereas the atactic and syndiotactic isomers are in thermodynamic environments that are worse than 'theta' conditions. Neutron reflectometry data have been analysed to give monolayer thickness and composition. At low surface concentrations, the layer thickness of the syndiotactic polymer increases to an eventually constant value although the surface pressure and concentration increase still further. For the isotactic polymer, the layer thickness is essentially constant over the range of surface concentrations investigated. Initially, the monolayers contain a considerable volume fraction of air, which decreases as the surface concentration increases. The monolayer thicknesses obtained are considerably larger than recent estimates from ellipsometry measurements, and possible sources for this discrepancy are discussed.

(Keywords: polymer monolayers; surface pressure; neutron reflectometry; interfaces; poly(methyl methacrylate))

INTRODUCTION

Polymeric molecules were among the first types of materials to be studied using a Langmuir film balance to ascertain the surface pressure–area (π/A) isotherms[1–3]. Although a considerable number and variety of polymers were investigated, quantitative interpretation of the data was sparse and in the main restricted to classification of isotherm type and evaluation of the limiting area per segment[4]. A notable exception to this early work is that of Schuler and Zisman on poly(ethylene oxide)[5]. Exact treatments of surface pressure at very low surface concentrations (Γ) have been given by Frisch and Simha[6] and independently by Huggins[7]. In the 'dilute' region, the surface pressure is describable by an equation of state:

$$\pi/RT = \Gamma/M + A_{22}\Gamma^2 + \cdots \quad (1)$$

where M is the polymer molecular weight and A_{22} is the second virial coefficient for the dependent in the interactions between the two-dimensional polymer molecules and between the substrate phase and the molecule. In common with polymer solutions in three-dimensional space, a large value of A_{22} indicates that the substrate is a good solvent and the polymer adopts an expanded conformation (relative to its two-dimensional unperturbed dimensions) on the surface.

In the development of renormalization-group theory and scaling-law descriptions of polymer solutions[8], the dimensionality of the system, d, is explicit in the equations for the dependence of osmotic pressure, radius of gyration, etc., on polymer concentration. Daoud and Jannink[9] and subsequently des Cloizeaux[10] obtained the general relationship (where Γ is in number of polymer chains per unit surface area):

$$A_{2d} \sim N^{\nu d}\tau^{d(\nu-\nu_\theta)\varphi_t} \quad (2)$$

where N is degree of polymerization, d is the dimensionality, ν is the exponent in the relation between radius of gyration R_g and N, i.e. $R_g \sim N^\nu$, ν_θ is the exponent for R_g at the theta temperature θ, $\tau = 1 - \theta/T$ and φ_t = crossover exponent (= 0.6 in two dimensions).

For good solvent conditions and $d = 2$, the generally accepted value of ν is 0.75[11]; the situation is not so clear for ν_θ. In the original scaling-law analysis a value of 0.505[12] was obtained for ν_θ and $d = 2$, but values up to 0.59 have also been obtained[13] by self-avoiding walk calculations. An exact value of 4/7 for ν_θ has been reported by Duplantier and Saleur[14]. The values of these exponents become highly relevant as the surface concentration Γ of the polymer in the monolayer is

* To whom correspondence should be addressed

0032-3861/91/183284-11

increased. Above the dilute region a new regime of behaviour is entered. In normal $d = 3$ solutions, the concentration above which this begins to happen is termed c^* and the molecules overlap to a certain extent and attenuate the intramolecular interactions[8,15]. The important length scale is the correlation length ξ, corresponding to the diameter of the blobs introduced by Daoud and Jannink[9]. It is difficult to envisage how such an interaction translates to two dimensions, and the fact that scaling-law behaviour is experimentally observed for polymer monolayers when $\Gamma > \Gamma^*$ may be evidence for them being only pseudo-two-dimensional. Above Γ^* then:

$$\pi/T \sim \Gamma^{\nu d(\nu d-1)}\tau^{(\nu-\nu_0)d/\Psi_1(\nu d-1)} \quad (3)$$

For a fixed temperature:

$$\pi \sim \Gamma^{y} \quad (4)$$

$$y = 2\nu/(2\nu - 1) \quad (5)$$

Continuing the analogy with solutions, at still higher concentrations of polymer on the surface of the substrate, there should exist a second concentration Γ^{**} at which the behaviour crosses into the concentrated regime where all intramolecular interactions are screened out and theta behaviour is expected. For this region at a fixed temperature:

$$\pi \sim \Gamma^{z} \quad (6)$$

$$z = 2\nu_\theta/(2\nu_\theta - 1) \quad (7)$$

From the details given above, the extremes of the values of the exponent y expected are between 3 for $\nu = 0.75$ and 101 for $\nu_\theta = 0.505$! There is one other important exponent corresponding to collapse of the polymer chain, in which case $\nu = \frac{1}{2}$ and the exponent becomes infinite.

Rondelez[16] was among the first to utilize π/Γ data to investigate experimentally this scaling-law analysis of polymeric monolayers, and a considerable amount of work in a similar vein was reported by Kawaguchi *et al.*[17–19]. Rondelez *et al.*[16] investigated poly(methyl methacrylate) (PMMA) spread at the air–water interface and from the π/Γ behaviour above Γ^* they obtained $\nu = 0.56$ at 289 K; subsequent repeated measurements[20] on this polymer gave $\nu = 0.53$ over the temperature range 274–309 K and moreover a negative value of A_{22} was noted at 289.5 K. This latter point was supporting evidence for the value of ν_θ being 0.57 rather than the scaling-law value of 0.505.

Kawaguchi *et al.* investigated poly(methyl acrylate) and polyethers[17–19]. For poly(methyl acrylate) above Γ^* they found $\nu = 0.51$ for $T = 291.2$ K, whereas for poly(ethylene oxide) at 295 K a value of 0.77 was extracted for ν. The value obtained for the poly(methyl acrylate) system has been questioned by Rondelez *et al.*[20], who repeated the measurements on the same polymer and obtained $\nu = 0.78$. Given the uncertainty of the physical nature of Γ^* for a polymer monolayer, some concern has been expressed about the accuracy and physical relevance of the exponents obtained from π/Γ isotherms above Γ^*. Recently, Rondelez[21] has addressed this problem by making π measurements at extremely low values of Γ and evaluating A_{22} for a series of molecular weights of PMMA. From these data at 288.5 K they obtained a mean value of ν of 0.55 ± 0.02 from the molecular-weight dependence of A_{22} and the dependence of π on Γ above Γ^*.

Although the improvement in the theoretical aspects of polymer monolayer surface pressure isotherms provides a rationale of the observed behaviour, an abiding problem is the structure and composition of the polymer monolayers. Very elegant methods of obtaining surface viscoelastic properties have been developed[22] but the authors comment[23] that physical interpretation is difficult owing to the absence of structural information on the polymer film. In the past[3] it has been conventional to assume complete monolayer formation and to calculate the film thickness from the bulk density of the polymer. This assumes the formation of a continuous, coherent film of uniform composition. Schuler and Zisman attempted some analysis of the nature and configuration of the poly(ethylene oxide) molecule at the air–water interface in their work[5]. Moreover, Huggins recognized that the absence of any structural information about polymers at the air–water interface was a serious hindrance to interpretation of values of A_{22}. Kim *et al.*[24] recently addressed this problem using ellipsometry and concluded that PMMA existed at the air–water interface as a series of 'condensed polymer islands'. The difficulty with ellipsometry is in the exact value of the refractive index used, and these results will be commented on later. Moreover, it is well known that the shape of π/Γ isotherms for PMMA are extremely dependent on the stereochemical composition of the molecule[4]. Apart from the work of Rondelez[21] this does not seem to have been greatly appreciated.

In this paper we combine data on π/Γ isotherms with the evaluation of monolayer thickness and composition from neutron reflectometry data for stereoisomers of PMMA at the air–water interface. Neutron reflectometry is a recent addition to the techniques for the analysis of surfaces and has already been applied to polymer solutions, solid polymer films and surfactants at the air–liquid and liquid–solid interfaces.

THEORY OF NEUTRON REFLECTOMETRY

Detailed discussions of the principles of specular reflection of neutrons, instrumental design and the use of multilayer optics methods of analysis are already available in the literature[25–28]. Only the salient points that have relevance to our data will be addressed here. Other applications have been discussed elsewhere[29].

Neutron reflectometry is the measurement of the intensity of the specularly reflected neutron beam as a function of the scattering vector $Q = (4\pi/\lambda)\sin\theta$ (λ = wavelength, θ = glancing angle of incidence of neutron beam on the surface) perpendicular to the reflecting surface. This intensity is related to the neutron refractive index (n) profile perpendicular to the surface and since:

$$n = 1 - (\lambda^2/2\pi)\rho \quad (8)$$

where ρ is the scattering length density, then the intensity of reflection depends on ρ. Reflection and refraction take place at each interface in the surface layer and the reflected beams interfere with each other. The form of the reflectivity profile obtained is determined by the Fresnel coefficients at each interface. These in turn are determined by the neutron refractive index (and hence

ρ) and the optical path length in the surface film, which is a function of the film thickness. For the analysis of neutron specular reflection profiles as a function of Q, a model has to be chosen that will utilize values of ρ, the film thickness and the number of multilayers in the film. The calculation method used here follows that of Abeles as described by Heavens[30] and permits the analysis of multilayers. Factors that influence the reflectivity profile are the scattering length density ρ of the film and the substrate together with the thickness t of the surface film. In the analysis of specular reflection data, these factors are usually adjustable parameters in the fitting of the expression for the reflectivity profile to the data[25]. These two factors are coupled in their action on the resultant reflectivity profile. However, the great benefit of neutron reflectometry is that by replacing protons by deuterium the reflectivity can be changed markedly, but since the physical chemistry of the system is not radically changed by deuterium labelling, the same physical model must fit both data sets. This change in scattering length density with proton replacement is particularly valuable for polymer monolayers at the air–water interface. Light water H_2O has a scattering length density of -0.562×10^{-6} Å^{-2} whereas that of D_2O is 6.34×10^{-6} Å^{-2}. Consequently these may be mixed in the correct proportion to give an aqueous substrate phase with $\rho = 0$, i.e. no specular reflection should be observed. Hence a monolayer spread on the surface of 'air-contrast-matched' water ($\rho_{air} = 0$) is observable in isolation of any reflectivity contributions from the interface. There is a contribution from background signal mainly due to incoherent scattering processes. This generally has no dependence on Q and is therefore flat and isotropic. Incoherent scattering is particularly evident in systems containing hydrogen owing to its large incoherent scattering cross section. As a consequence the background signal can be relatively large even in air-contrast-matched water owing to the presence of H_2O. At high values of Q where the reflectivity of the surface layers becomes small, incoherent scattering can obscure the features of the specular reflection profile.

EXPERIMENTAL

Polymers

The free-radically polymerized deutero polymer dPMMA was a generous gift from Dr D. J. Walsh of Du Pont, Wilmington, Delaware, USA, and had a molecular weight of $\sim 10^7$. The hydrogenous polymer hPMMA was a fraction from a broad distribution sample from the Rubber and Plastics Research Association, Shawbury, UK. Syndiotactic dPMMA was prepared by anionic polymerization of the deutero polymer under high vacuum. The polymerization was carried out in tetrahdrofuran (THF) at -78°C using 9-fluorenyl-lithium as initiator. After terminating the reaction by addition of degassed methanol, the polymer was recovered by precipitation in methanol and vacuum drying. An exactly similar procedure was used to prepare syndiotactic hPMMA. Isotactic dPMMA and hPMMA were purchased from Polymer Laboratories Ltd, Church Stretton, UK. All polymers were analysed by size exclusion chromatography and ^{13}C n.m.r. using a 400 MHz spectrometer. The results of these analyses are given in *Table 1*.

Surface pressure–area isotherms

Surface pressure data were obtained using a NIMA surface film balance (NIMA Technology, Coventry, UK). This consisted of a circular Teflon trough with motorized barriers, thermostated by water circulated

Table 1 Characterization data for poly(methyl methacrylate) specimens used

(a) Molecular weights from size exclusion chromatography

Polymer	$\bar{M}_w/10^3$	$\bar{M}_n/10^3$	$\bar{M}_w/\bar{M}_n$
dPMMA(r)			
hPMMA(r)	114.0	97.0	1.17
dPMMA(s)	119.0	335.0	2.81
hPMMA(s)	267.0	151.0	1.77
dPMMA(i)	26.6		6.5
hPMMA(i)	19.0		4

(b) Relative integral signal intensity for tactic sequences in ^{13}C n.m.r. spectra

	Fraction of total n.m.r. signal				Proportion in molecule	
Polymer	mmmm	rmrr/mmrr	rrrr	mrrr	r	m
hPMMA(r)	0	0.42	0.36	0.22	0.79	0.21
dPMMA(r)	0					
hPMMA(s)	0	0.32	0.56	0.12	0.85	0.15
dPMMA(s)	0	0.24	0.60	0.16	0.87	0.13
hPMMA(i)	0.84	0	0.16	0	0.16	0.84
dPMMA(i)	1.00	0	0	0	0	1.00

from an external thermostat. The surface pressure was monitored by a Wilhelmy plate attached to a sensitive force transducer, and the data were displayed in real time by the controlling computer. Data were stored in the form of surface pressure and area, and were subsequently manipulated to produce surface pressure as a function of surface concentration (Γ/mg m^{-2}). Solutions of each polymer were made in chloroform at a concentration of $\sim$0.1 mg ml^{-1} and dispensed on to the subphase surface in the trough using a microlitre syringe. Typically the initial mass of polymer deposited was $\sim$30 μl $\times$ 1 mg ml^{-1} (accurately known); the initial area being 950 cm^2, this gives a starting surface concentration (Γ) of around 0.3 mg m^{-2}.

Neutron reflectometry

Neutron reflection profiles were obtained using the CRISP instrument at the UK pulsed neutron source ISIS at the Rutherford–Appleton Laboratory. This instrument has been fully described elsewhere[26] and its application to other surface and interfacial problems has been reported[29]. Briefly, a 'white' neutron beam directed at a fixed angle to the horizontal is collimated before being incident on the specimen surface. The reflected beam is collected by a detector and analysed for the variation of reflected intensity as a function of scattering vector Q by time-of-flight methods. For our experiments a rectangular Langmuir trough (34 cm $\times$ 20 cm) constructed from Teflon was placed on a vibrationless table in the neutron beam, the long dimension of the trough being in line with the beam axis of the reflectometer. The active area of the trough was enclosed in a close-fitting aluminium and Perspex box with entrance and exit windows for the neutron beam cut in the aluminium. These windows were covered with quartz plates. After mounting in the beam, the trough was filled with the subphase liquid and swept clean by repeated movement of two motorized barriers to the trough centre and suction of the subphase surface. The barriers were then set at their maximum separation and the polymer solution dispensed through a hole in the top of the enclosing box. After allowing the dispensing solvent to evaporate, the hole was resealed. By moving the barriers, the polymer film could be compressed, increasing Γ, and thus neutron reflection profiles at a series of surface concentrations were obtained without the need to sweep the surface clean and reload. Two subphase polymer combinations were used in the experiments reported here. First all hydrogenous polymers were investigated when spread on D_2O; secondly all deuterated polymers were investigated when spread on air-contrast-matched water (a.c.m.w.). This latter subphase consists of a mixture of 8.9% D_2O and 91.1% H_2O by weight.

RESULTS

Surface pressure–surface concentration isotherms

The variation of surface pressure (π) with surface concentration (Γ) for each stereotactic polymer is presented in *Figure 1*. Clear differences are observable in the isotherm for isotactic PMMA compared to those for the remaining two polymers. For the former polymer, the surface pressure displays an immediate increase as Γ increases, and a definite transition to a smaller dependence of π on Γ takes place at $\Gamma \simeq 1.5$ mg m^{-2}.

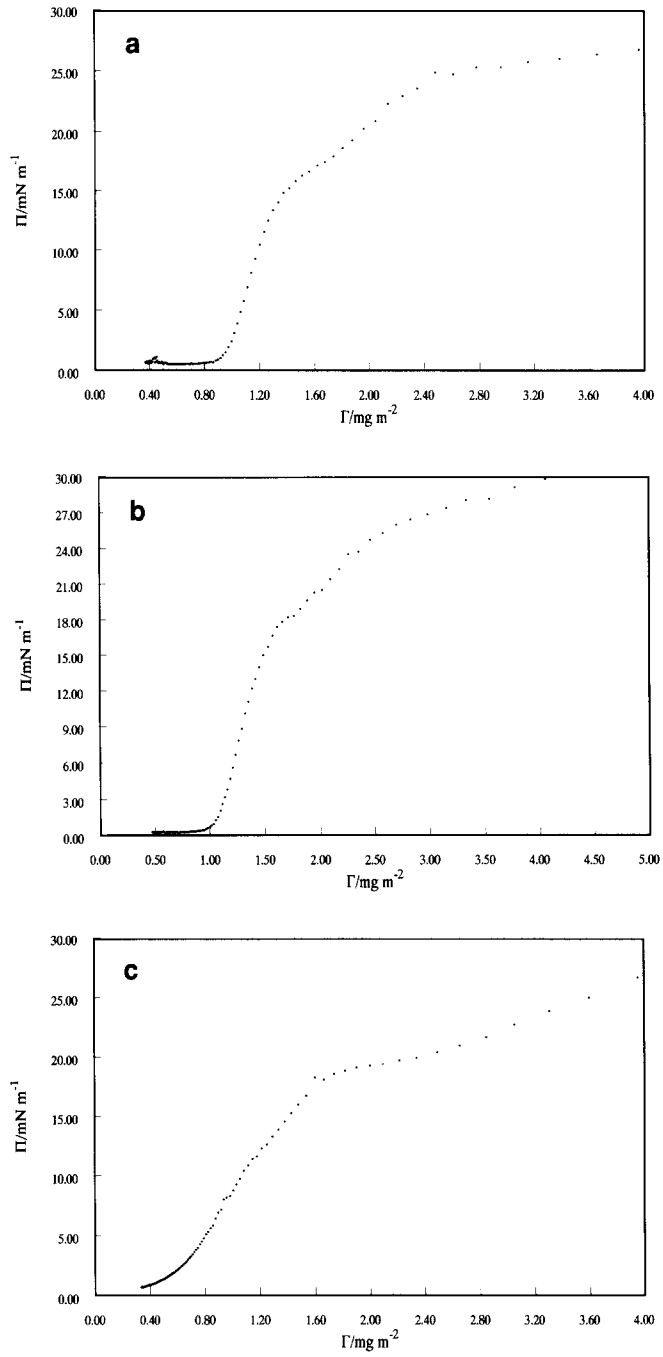

Figure 1 Surface pressure isotherms for (a) atactic, (b) syndiotactic and (c) isotactic poly(methyl methacrylate) spread at the air–water interface at 298 K

Both atactic and syndiotactic have very similar isotherms, which, in view of their near-identical stereochemical unit content, is not surprising. Limiting areas per segment calculated from extrapolation of data in *Figure 1* gave values of 15–16 Å^2/segment for the atactic and syndiotactic polymers. This value is in agreement with the early reported values[8] and with values obtained by using the data of Rondelez *et al.*[16,20]. By contrast the limiting area for the isotactic polymer is $\sim$32.0 Å^2/segment. Although the molecular weights of the polymers used are markedly different, it has been remarked that asymptotic values of such properties as limiting area are obtained for molecular weights of $\sim$10000 and above, and consequently these differences in limiting area are solely attributable to the stereotacticity of the PMMA specimens.

At low values of Γ, the polymer molecules on the surface behave as isolated species and the surface pressure can be described by an equation of state (equation (1)). Consequently, by using equation (1) values of A_{22} can be obtained from π/Γ data. Such measurements have been reported by Rondelez[21] for an atactic PMMA, but the data from our trough system for $\Gamma \leqslant 0.5$ mg m^{-2} are insufficiently accurate and it is this region of Γ which is needed for evaluation of virial coefficients. Although the surface pressure data at very low Γ values cannot be used to evaluate A_{22} and M_n, it is clear that isotactic PMMA (iPMMA) has a positive A_{22} whilst those of atactic PMMA (aPMMA) and syndiotactic PMMA (sPMMA) are negative. *Figure 2* shows plots of π/Γ as a function of Γ in the low-Γ region, which clearly show the difference in behaviour of the two stereochemical forms of the polymer.

Values of the exponent v for each of the polymers used were extracted from double logarithmic plots of π and Γ (*Figure 3*). The crossover concentration Γ^* is easily identifiable for aPMMA and sPMMA as the intersection of lines through the horizontal data points at low Γ and those data points with a strong dependence on Γ. For iPMMA, there is a strong dependence of π on Γ from the outset, but a value of Γ^* is discernible from the data. The values of Γ^* and the slope of the semi-dilute region (y in equations (4) and (5)) are given in *Table 2*, which also includes values of the crossover concentration Γ^{**} to the concentrated region and the slope of the π/Γ plot (z in equations (6) and (7)) in this region.

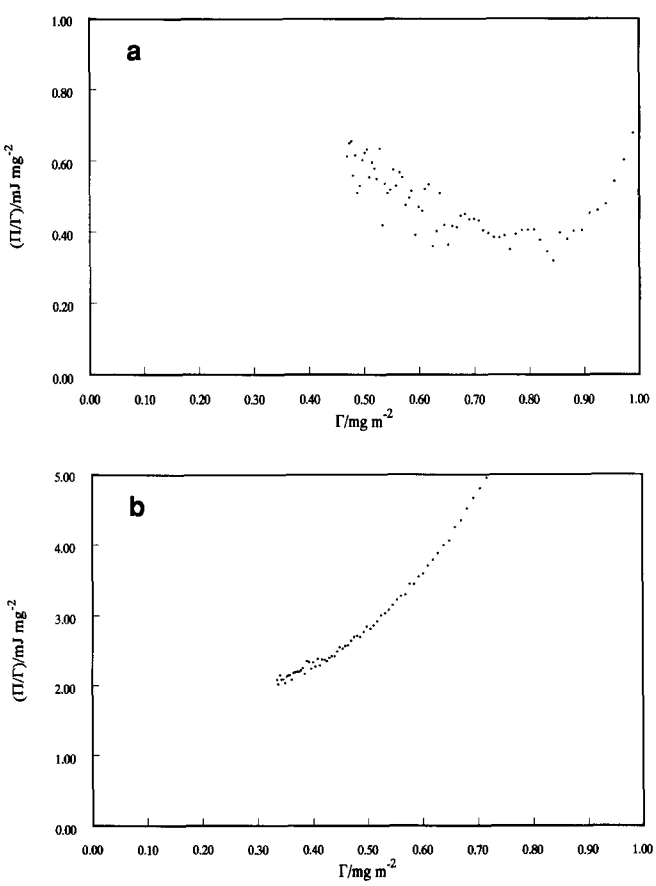

Figure 2 Plot of π/Γ as a function of Γ for (a) syndiotactic and (b) isotactic poly(methyl methacrylate)

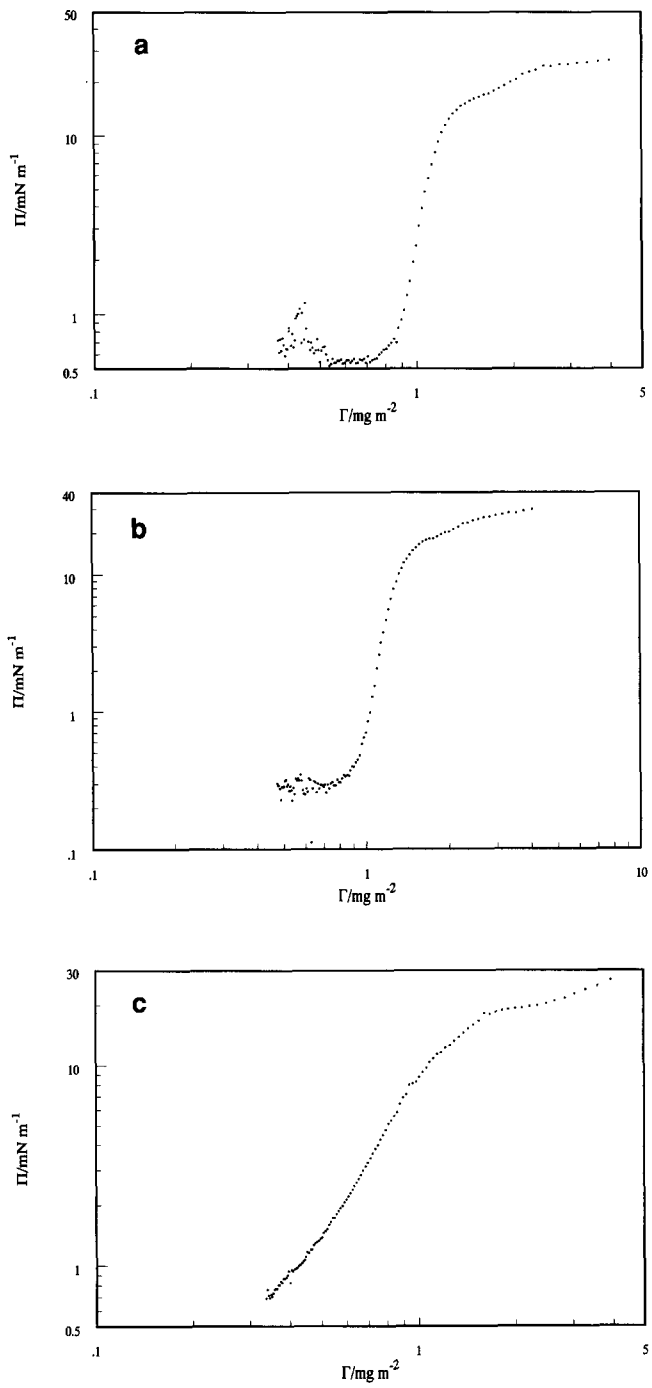

Figure 3 Double logarithmic plots of the data in *Figure 1*; a, b and c refer to the same polymers as in *Figure 1*

Table 2 Values of Γ^*, Γ^{**}, y and z from double logarithmic plots of π and Γ

Polymer	Γ^* (mg m^{-2})	y	Γ^{**} (mg m^{-2})	z
hPMMA(r)	0.93	9.79	1.33	1.54
dPMMA(r)		9.58		
hPMMA(s)	0.99	31.46	1.45	0.62
dPMMA(s)	1.06	11.98	1.46	0.88
hPMMA(i)	0.53	2.77	1.43	0.62
dPMMA(i)	0.62	2.82	1.53	0.38

Neutron reflectometry

Measured neutron specular reflection profiles obtained for the syndiotactic and isotactic deutero poly(methyl methacrylates) are shown in *Figures 4* and *5*. Both sets of reflection profiles show similar characteristics: as Γ increases, the reflectivity at low Q values increases; moreover the dependence of the reflectivity becomes more pronounced with increased Γ. At high Q values ($Q > 0.35$–0.4 Å^{-1}), the reflectivities have a constant background value, the level of which is determined by the composition of the subphase. The variation in specular reflection for hydrogenous polymer spread on D_2O is shown in *Figure 6*. The changes here are much more subtle and a lower background reflectivity compared to air-contrast-matched water is also apparent. This latter observation is due to the lower quantity of nuclei present with large incoherent scattering cross sections when compared to the light water containing air-contrast-matched subphase. The differences in the reflection profile are understandable if the concept of the layer and subphase acting as barriers that the neutron has to surmount is used. *Figure 7* shows schematic sketches of the situation for hPMMA spread on D_2O and dPMMA spread on a.c.m.w. In the latter case, the polymer layer is a large perturbation of the scattering length density of the surrounding media. For the hydrogenous polymer, the perturbation is much less significant owing to the large scattering length density of D_2O. Examples of the fits to the specular reflection profiles are shown in *Figure 8* for polymer spread on D_2O and a.c.m.w. For each polymer–subphase combination the data were fitted by modelling the monolayer as a smooth homogeneous slab at the surface. Values of the reflectivity at large Q were used to fix the background signal, and a least-squares fit to the data was performed where both thickness t and scattering length density ρ were the adjustable parameters. The values obtained were used as initial estimates in the subsequent refinement of the fits. For this purpose the value of the layer thickness was fixed at some arbitrary value in the region of the initial fit and the least-squares fit evaluated again with only ρ as the adjustable parameter. The residual between the fit and the data was noted and the procedure repeated for a different value of the thickness. Values of the residuals were plotted as a function of the thicknesses and the optimum value of t identified as where the minimum of the residual curve occurred. *Figure 9* shows

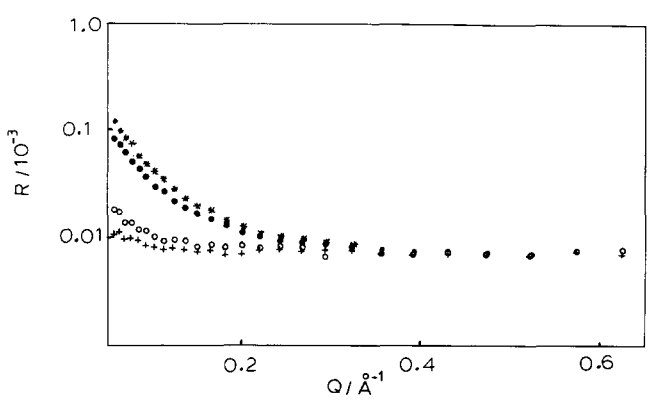

Figure 4 Neutron reflectometry profiles obtained for isotactic deutero poly(methyl methacrylate) spread on air-contrast-matched water. Surface concentrations (mg m^{-2}): (*) 1.0, (●) 0.8, (○) 0.4, (+) 0.2

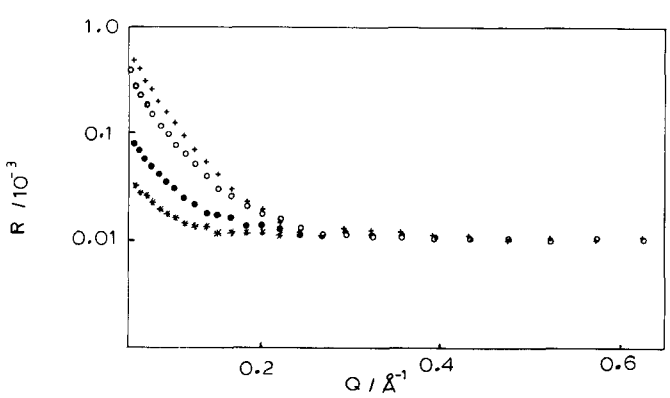

Figure 5 Neutron reflectometry profiles for syndiotactic deutero poly(methyl methacrylate) on air-contrast-matched water. Surface concentrations (mg m^{-2}): (+) 2.0, (○), 1.0, (●) 0.6, (*) 0.3

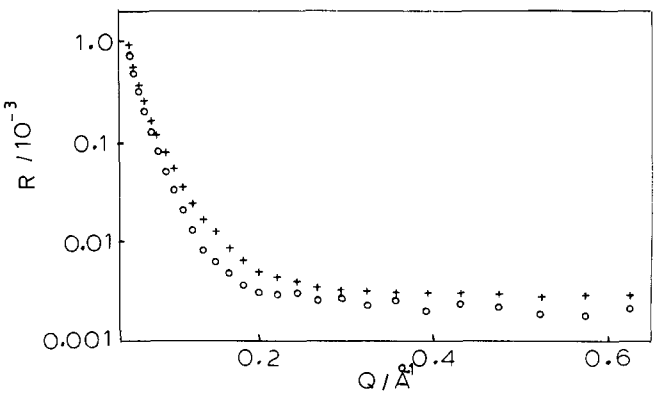

Figure 6 Typical neutron reflectometry profiles for atactic hydrogenous poly(methyl methacrylate) spread on D_2O. Surface concentration (mg m^{-2}): (○) 4.95, (+) 0.1

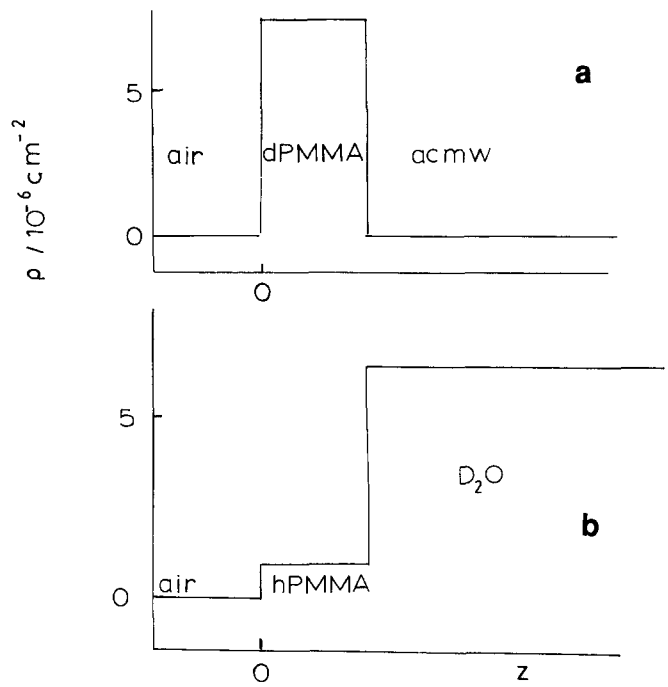

Figure 7 Schematic sketches of scattering length density variation across the air–polymer–water interface. The ideal case of a pure polymer film is shown here. (a) Deutero PMMA on air-contrast-matched water. (b) Hydrogenous PMMA on D_2O. The distance normal to the interface is denoted by z

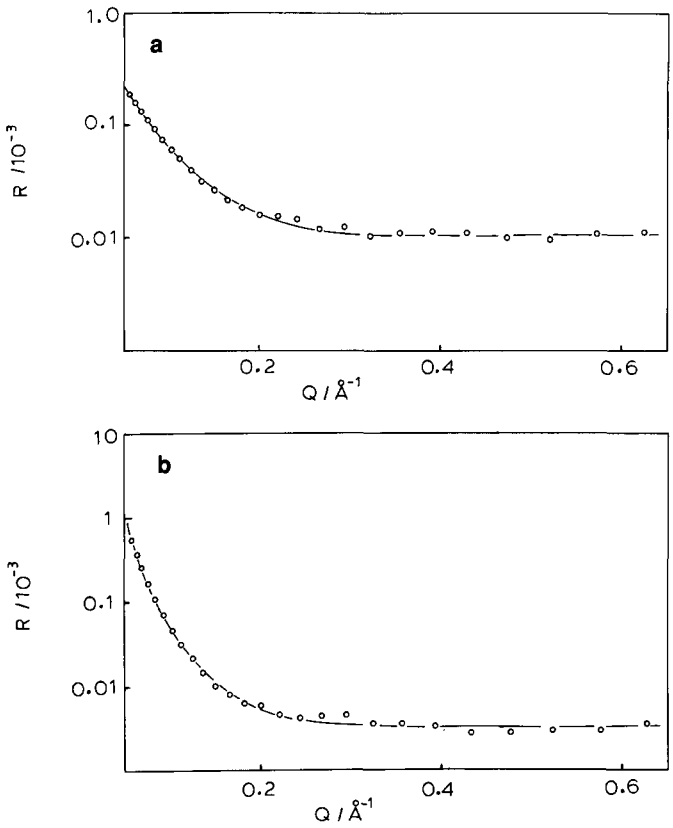

Figure 8 Representative fits (full curves) to reflectometry data for (a) deutero sPMMA on air-contrast-matched water and (b) hydrogenous sPMMA on D_2O

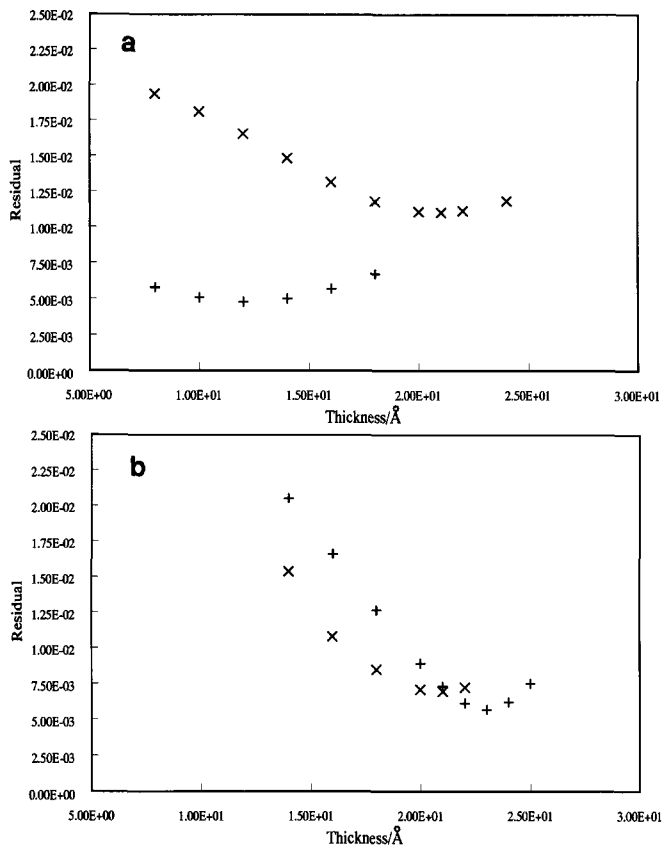

Figure 9 Plots of residuals between model fit and reflectometry data as a function of layer thickness for syndiotactic polymer: (a) 0.6 mg m^{-2}, (b) 1.5 mg m^{-2}; (+) deutero polymer, (×) hydrogenous polymer

Table 3 Monolayer thicknesses t and scattering length densities ρ^a from neutron reflectometry

	aPMMA			sPMMA			iPMMA		
Γ (mg m^{-2})	t (Å)	ρ_{acmw}	ρ_{D_2O}	t (Å)	ρ_{acmw}	ρ_{D_2O}	t (Å)	ρ_{acmw}	ρ_{D_2O}
0.1									
0.2	18	0.64		12	0.8	0.43	0.29	0.25	0.44
0.3				20	1.07		16	0.8	0.63
0.4				20	1.25	0.72	16	0.93	0.59
0.5	17	2.05	0.87	18	1.70		22	0.68	0.49
0.6				16	2.44	0.98	19		0.52
0.75	15	3.57							
0.8				18	3.5	1.02	16	2.67	0.82
1.0	18	3.76	1.24	20	3.86	1.04	15	3.19	0.84
1.23	17	4.04							
1.5				22	4.60	1.06	17	2.60	0.87
1.7	17	4.15							
2.0	17	3.91	1.85	23	4.54	1.26			
2.5	19	4.22							
3.5	21	4.59	1.69						
4.95	22	5.31	1.69						

[a] ρ_{acmw} and ρ_{D_2O} are the scattering length densities (10^{-6} Å^{-2}) for the deutero polymer on air-contrast-matched water subphase and hydrogenous polymer on D_2O respectively

such a plot of residuals for both hydrogenous and deuterated polymers. There are a few points to note. First, the minima are not in the same place, the disparity becoming less evident at higher surface coverages. Secondly, the minima were shallower for the lower surface coverages. Because of the disparity in value of t where the minima were observed, a value of t halfway between the value for the deutero and hydrogenous polymers was chosen. The least-squares fits were then re-evaluated for both isotropes of PMMA, constraining the thickness to this average value. *Table 3* reports the values of t and ρ obtained by this method for all combinations of polymer and subphase investigated in this work.

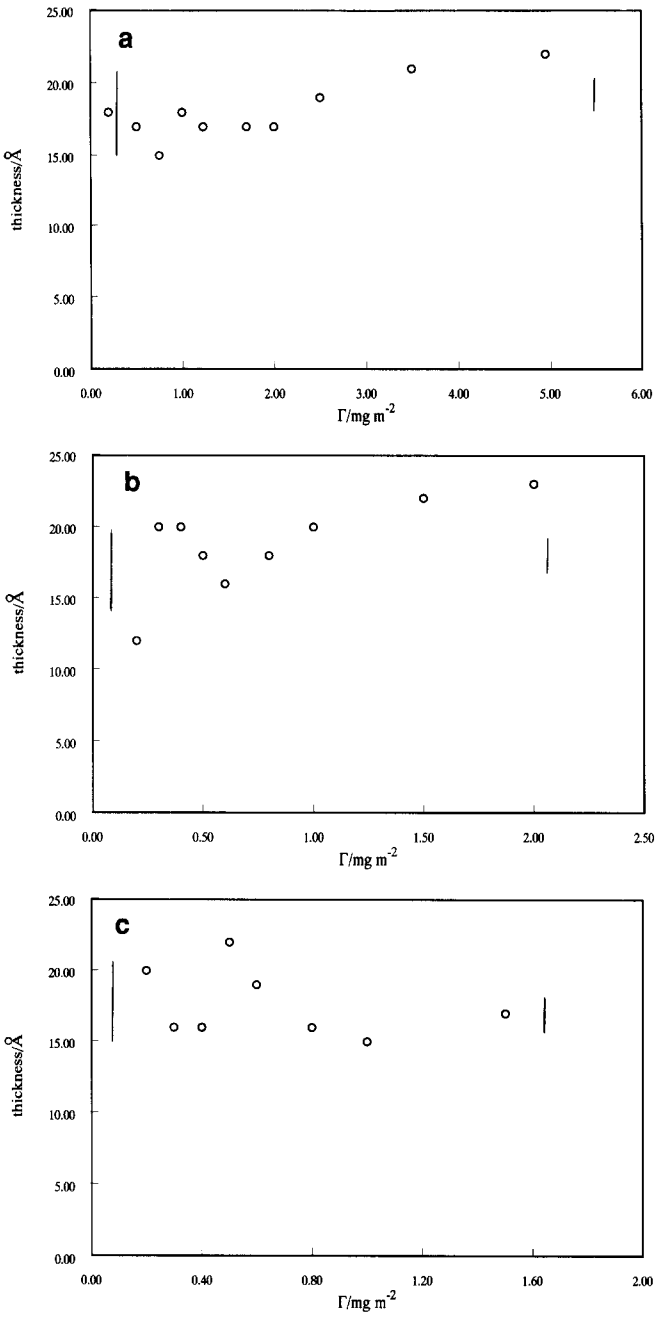

Figure 10 Dependence of monolayer thickness from neutron reflectometry on surface concentration: (a) aPMMA, (b) sPMMA, (c) iPMMA. Vertical lines indicate extent of uncertainty in layer thickness from residuals analysis

As *Figure 10* shows, iPMMA forms a monolayer of essentially constant thickness of ~18 Å over the range of Γ studied. Over this same range of Γ, sPMMA increases in thickness from ~10 to 25 Å. Up to a surface concentration of 2.0 mg m^{-2}, the atactic polymer has a constant layer thickness of ~18 Å; thereafter there is a step change in thickness to an asymptotic value of 21 Å. Discussion of the variation in ρ with surface concentration is dealt with below, where the values of ρ have been used to determine the composition of the PMMA monolayers.

DISCUSSION

A noticeable feature of the values of y obtained (*Table 2*) from the π/Γ isotherms is their wide range. What appears to be particularly disturbing is the discrepancy between the y values for the deutero and hydrogenous PMMA, this being a factor of 3 for sPMMA. However, in this region of y, the value of ν does not change rapidly, as *Figure 11* shows. From the values of y obtained, ν exponents of 0.55_7, 0.52 (± 0.02) and 0.78 were evaluated for the atactic, syndiotactic and isotactic PMMA molecules respectively. Evidently isotactic PMMA appears to be in a good solvent situation when spread on water, whereas both the atactic polymer and the syndiotactic polymer are in less than theta states if the value of 0.57 is accepted for ν_θ. The fact that we obtain negative A_{22} values for these two polymers at 298 K is support for the view that ν_θ cannot be as low as 0.505 and must be greater than 0.55. From our values it seems that the syndiotactic polymer is nearer collapsed-chain conditions than theta conditions.

The values of ν obtained for sPMMA and iPMMA may be related to the layer thicknesses observed. For iPMMA, the value of ν suggests a highly favourable thermodynamic interaction between water and polymer segments. Consequently, to maximize this interaction the polymer molecule will extend to produce a thinner layer. By contrast, sPMMA, being nearer collapse, will adopt configurations that reduce contacts between polymer and subphase. This can be achieved if the sPMMA segments surround themselves with like segments leading to a thicker monolayer. If this view is correct, it implies that the sPMMA monolayer should have a higher content of polymer with minimal content of the subphase.

A priori the polymer monolayer at the air–water interface could contain three components, polymer, water and air. The scattering length density obtained of this composite layer is the volume fraction weighted sum of the scattering length densities of each component:

$$\rho = \Phi_a \rho_a + \Phi_p \rho_b + \Phi_w \rho_w$$

where Φ_i = volume fraction of component i and the subscripts a, p and w denote air, polymer and water respectively. For the polymer spread on a.c.m.w., then $\rho_a = \rho_w = 0$ and hence:

$$\rho = \Phi_p \rho_p$$

Consequently, the volume fraction of the polymer in the monolayer can be obtained directly from the ratio of the measured scattering length density to that of the bulk polymer. The same process can be used for the

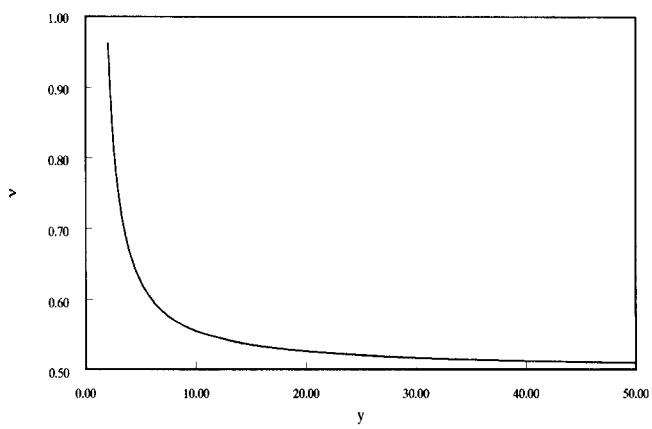

Figure 11 Calculated dependence of ν, the excluded-volume exponent, on y, the slope of π as a function of Γ for $\Gamma^* < \Gamma < \Gamma^{**}$

hydrogenous polymers spread on D_2O. In this situation:

$$\rho = \Phi_p \rho_p + \Phi_w \rho_w$$

Since Φ_p is known from the a.c.m.w. data and ρ_w and ρ_p are calculable, then:

$$\Phi_w = (\rho - \Phi_p \rho_p)/\rho_w$$

The volume fraction of air in the monolayers is simply obtained by the difference of the sum of Φ_p and Φ_w from unity. Values of the volume fraction of the three components in the monolayers obtained by these calculations are given in *Figure 12* as a function of Γ. It is clearly evident that the sPMMA layer does have a higher content of polymer than the iPMMA at the same value of Γ. Surprisingly, the water content does not appear to be vastly different for the two polymers given their very different interaction thermodynamics. It is also noteworthy that the iPMMA contains a significant volume fraction of air, whereas for the sPMMA the air content is much lower and for the atactic polymer it is zero at high values of Γ. Overall, the atactic polymer displays properties that are essentially those of sPMMA, although its thickness variation with Γ seems to resemble iPMMA. In this respect the magnitude of the error bars on *Figure 10* are worthy of comment. The size of the error bar reflects the distance separating the positions of the minima in the residual curves discussed earlier. At low values of Γ, the error bars are large and consequently the values of t should be viewed in the light of this fact. We estimate the error in the values of the scattering length density to be of the order of 5–7%.

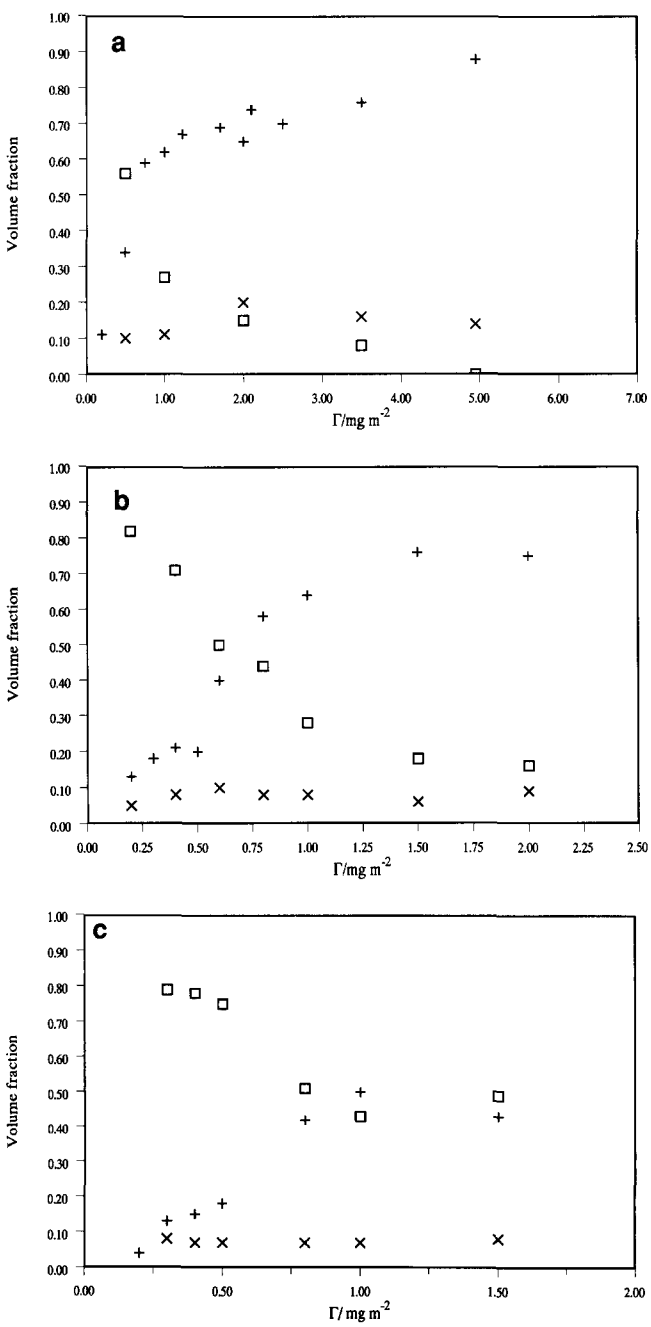

Figure 12 Volume fraction composition of polymer monolayers as a function of Γ: (a) atactic, (b) syndiotactic, (c) isotactic; (+) polymer, (□) air, (×) water

In fitting the reflection profiles, it is the product, $t\rho$, that occurs in the equations for the reflectivity. Hence although the uncertainty in the individual values of t and ρ may be large, the error in their product will be considerably smaller. The uniqueness of the model chosen can be tested by using the value of $t\rho$ to calculate the value of the surface concentration Γ_c, and to compare this with the value dispensed on the surface. Values of Γ_c calculated by the relation:

$$\Gamma_c = m\rho t / N_A \sum b_i$$

where m is the monomer unit molecular weight, N_A is Avogadro's number and $\sum b_i$ is the sum of the atomic coherent scattering lengths in the monomer unit.

The results of these calculations are compared with the values of Γ dispensed in *Figure 13*. For the syndiotactic polymer the agreement between the two values is reasonable and in parts excellent. For the iPMMA the values of Γ_c are always less than the experimental value and this is particularly evident at high values of Γ, where the discrepancy approaches some 50%. Since it appears that the neutron beam 'sees' all of the sPMMA ($\Gamma_c \simeq \Gamma$), then this suggests that all of this polymer rests on the surface of the subphase. For the iPMMA, it seems as if some of the polymer has disappeared. In view of the very favourable thermodynamics (as indicated by the v value) for this polymer, it is probable that some of the molecule is immersed in the subphase, presumably as loops or tails, which may extend for very long distances into the subphase. These components of the surface film are probably so dilute that we are not able to improve the model fit to the data by using a two-layer model. Additionally, to observe such a second layer, the reflectometry would need to be extended to much lower Q values to probe the longer distances normal to the interface. There may be some significance in the observation that the discrepancy between calculated and actual surface concentration becomes very marked at the point where the abrupt phase transition is observed in the π/Γ isotherm.

Owing to the grazing angles of incidence used in neutron reflectometry, the illuminated area used here was ~15 cm long by 4 cm wide. Consequently, the description provided is the average surface layer composition and thickness. Evidently, the sPMMA is all in the air phase, but we cannot say whether the air content is actually dissolved in the polymer monolayer or if there are islands of polymer separated by intervening polymer-free water surface. This is the view Kim *et al.*[24] arrived at from ellipsometry results. They were forced to assume a Lorentz–Lorenz average (polymer and water)

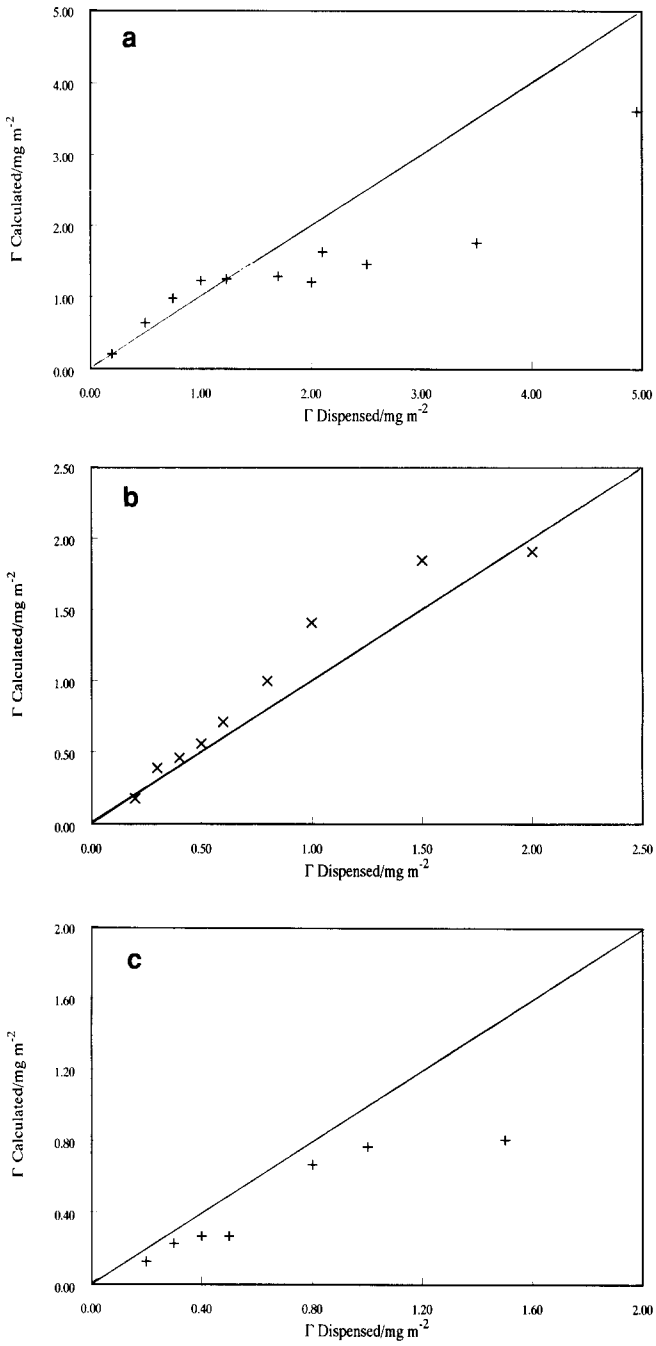

Figure 13 Calculated surface concentration of polymer (Γ_c) as a function of the experimental surface concentration Γ: (a) atactic, (b) syndiotactic, (c) isotactic. The lines are for $\Gamma_c = \Gamma$

of the monolayer refractive index in the absence of any compositional information. Evidently, the fact that air is incorporated in the film will considerably influence the refractive index. They calculate a monolayer thickness of 14 Å at $\Gamma = 2.3$ mg m^{-2} (which they define as the point where the fractional coverage is unity), which is considerably smaller than our values of ~18–20 Å at the same value of Γ. The stereotacticity of their PMMA is not stated, which prevents a meaningful comparison of their data with ours.

It is known that iPMMA forms helices in the crystalline state. One speculation may be that the air–water interface may promote helix formation, thus giving rise to the constant thickness of the polymer layer. The helix formation, if it exists, cannot be perfect since some of the polymer appears to be in the subphase. This polymer could be chain ends or fragments connecting helically coiled regions on the same molecule. The majority of the helical regions must be in the air phase since the air content of these monolayers is so high.

CONCLUSIONS

Considerable variation in the surface pressure isotherms of the different tactic forms of poly(methyl methacrylate) has been rationalized by the different thermodynamic nature of water to each of the polymers. These conclusions have been obtained from the slopes of the dependence of log π on log Γ for $\Gamma > \Gamma^*$. In common with Rondelez *et al.*, we observe negative two-dimensional second virial coefficients (A_{22}) for atactic and syndiotactic poly(methyl methacrylate), but our film balance is insufficiently accurate to produce values for A_{22} in the low region of Γ values required. By utilizing the different scattering length densities of hydrogen and deuterium, neutron reflectometry has been used to obtain unambiguous values of the monolayer thickness and scattering length density as a function of surface concentration of polymer. These data have enabled the calculation of the composition of the monolayer in terms of air, water and polymer content. This information is unobtainable by other techniques.

These data and calculated values of surface concentration from thickness and monolayer scattering length densities suggest that syndiotactic poly(methyl methacrylate) is located at the surface of the water phase with all of the polymer in the air phase. The isotactic poly(methyl methacrylate) has a constant layer thickness but some of the polymer appears to be immersed in the subphase. A possible explanation for the constant layer thickness of this latter polymer has been put forward in terms of formation of helical structures at the air–water interface. However, confirming evidence for this speculation has yet to be obtained.

ACKNOWLEDGEMENTS

We thank the Science and Engineering Council for making available funds to purchase the film balance and providing the neutron beam facilities at ISIS. JAH is also grateful to them for the provision of a maintenance grant.

REFERENCES

1 Crisp, D. J. *Colloid Sci.* 1946, **1**, 49
2 Crisp, D. J. *Colloid Sci.* 1946, **1**, 161
3 Parker, J. and Shereshefsky, J. C. *J. Am. Chem. Soc.* 1954, **58**, 851
4 Crisp, D. J. in 'Newer Methods of Polymer Characterization' (Ed. B. Ke), Wiley, New York, 1964
5 Schuler, R. L. and Zisman, W. A. *J. Phys. Chem.* 1970, **74**, 1523
6 Frisch, H. L. and Simha, R. *J. Chem. Phys.* 1957, **27**, 702
7 Huggins, M. L. *Kolloid Z.* 1973, **251**, 449
8 de Gennes, P. G. 'Scaling Concepts in Polymer Physics', Cornell University Press, London, 1979
9 Daoud, M. and Jannink, G. *J. Physique* 1976, **37**, 973
10 des Cloizeaux, J. *J. Physique Lett.* 1980, **41**, 151
11 Le Guillou, J. C. and Zinn-Justin, J. *J. Physique. Lett.* 1985, **18**, 1461
12 de Gennes, P. G. *J. Physique Lett.* 1978, **39**, 299
13 Douglas, J. F., Cherayil, B. J. and Freed, K. F. *Macromolecules* 1985, **18**, 2455
14 Duplantier, B. and Saleur, H. *Phys. Rev. Lett.* 1987, **59**, 539

15 Jeffers, E. and Edwards, S. F. *J. Chem. Soc., Faraday Trans. II* 1979, **75**, 1020
16 Vilanove, R. and Rondelez, F. *Phys. Rev. Lett.* 1980, **45**, 1502
17 Kawaguchi, M., Komatsu, S., Matsuzumi, M. and Takahashi, A. *J. Colloid Interface Sci.* 1984, **102**, 356
18 Kawaguchi, M., Yoshida, A. and Takahashi, A. *Macromolecules* 1983, **16**, 956
19 Takahashi, A., Yoshida, A. and Kawaguchi, M. *Macromolecules* 1982, **15**, 1196
20 Vilanove, R., Poupinet, D. and Rondelez, F. *Macromolecules* 1988, **21**, 2880
21 Poupinet, D., Vilanove, R. and Rondelez, F. *Macromolecules* 1989, **22**, 2491
22 Earnshaw, J. C. *Thin Solid Films* 1983, **99**, 189
23 Sauer, B. B., Kawaguchi, M. and Yu, H. *Macromolecules* 1987, **20**, 2732
24 Sauer, B. B., Yu, H., Yazdanian, M., Zografi, G. and Kim, M. W. *Macromolecules* 1989, **22**, 2332
25 Penfold, J. Rutherford–Appleton Laboratory Report, RAL-88-088, 1988
26 Penfold, J., Ward, R. C. and Williams, W. G. Rutherford–Appleton Laboratory Report, RAL-87-014, 1987
27 Rennie, A. R., Crawford, R. J., Lee, E. M., Thomas, R. K., Crowley, T. L., Roberts, S., Qureshi, M. S. and Richards, R. W. *Macromolecules* 1989, **22**, 3466
28 Lekner, J. 'Theory of Reflection', Nijhof, Dordrecht, 1987
29 Penfold, J. and Thomas, R. K. Rutherford–Appleton Laboratory Report, RAL-89-057, 1989
30 Heavens, O. S. 'Optical Properties of Thin Films', Butterworths, London, 1955